Journal of Radioanalytical and Nuclear Chemistry (2022) 331:5027–5032
https://doi.org/10.1007/s10967-022-08480-1

Method for calculating radon activity and radon rejection using a beta-gamma detector

Michael F. Mayer[1] · Matthew W. Cooper[1] · James H. Ely[1] · James C. Hayes[1]

Received: 21 April 2022 / Accepted: 3 August 2022 / Published online: 29 August 2022

Abstract
Radon interferes with concentration measurements used by atmospheric radioxenon systems. We demonstrate a method to quantify the amount of radon that is present in the detectors, the impact of radon activity on the minimum-detectable-concentrations, and how to determine the needed radon rejection levels. An example calculation shows a radon rejection level of 10^5 is sufficient to limit impact on the detector sensitivity. We anticipate this method will give analysist a better understanding of radon present in their measurements and allow system designers to tailor their systems' radon rejection better for its location.

Keywords Radioxenon · Radon · Radon rejection

Introduction

Radon is an impairing background for atmospheric monitoring systems that measure radioxenon activities from nuclear explosions. The systems collect atmospheric air samples for periods of 6 h, 12 h, or 24 h and then process the air to extract and purify xenon [1–4]. The samples are then measured using radiation detectors for 12 or 24 h. Occasionally, a few radon atoms may be present in the purified xenon sample. When this happens, the radon can negatively impact the xenon detection sensitivity [i.e., the minimum-detectable-activity (MDA) and minimum-detectable-concentration (MDC)]. As more radon is introduced to the detectors, the MDA and MDC for radioxenon increases. Because every atom of radon is radioactive, a small amount of radon will also interfere with the radioxenon signals. Currently, radon present in the samples is not quantified by the net-count method; nor is the rejection level needed predictively predetermined when the system is designed.

An activity measurement requires both an accurate account of detected events from a radionuclide and the detector efficiency. Presented in this work are the equations which relate the counts from radon's daughter particles to radon using the Bateman equations,[1] the simulations to show the fractional abundance of each daughter of radon in a detector cell, and a method to determine the efficiency of the detector. Using the fractional abundance and the efficiency, a radon activity equation is formulated. The radon activity is then used to determine expected MDC levels over a range of radon rejection levels and radon activities to determine optimal radon rejection levels for a system.

Background

Radon is an issue regardless of location. The isotopes of radon, ^{220}Rn (thoron) and ^{222}Rn (radon), are daughter products from ^{238}U and ^{232}Th, which are some of the largest naturally-occurring background sources and can be found anywhere in the world [5]. Thoron, which has a short half-life ($T_{1/2} = 55.6$ s), quickly decays away during the collection period leaving behind only its progeny while radon (^{222}Rn), which has a longer half-life ($T_{1/2} = 3.82$ d), is the form that will be observed in collected samples. Radioxenon monitoring systems normally reject radon by filtering out the particulate progeny and use gas absorption and elution to remove the radon gas. Thus, the daughters are filtered, and processing is long enough that most of the short-lived ^{220}Rn will never make it to the detector. The longer-lived radon isotope, ^{222}Rn, will remain in the collected sample

✉ Michael F. Mayer
michael.mayer@pnnl.gov

[1] Pacific Northwest National Laboratory, 902 Battelle Blvd, Richland, WA, USA

[1] See the Supplementary information for these equations.

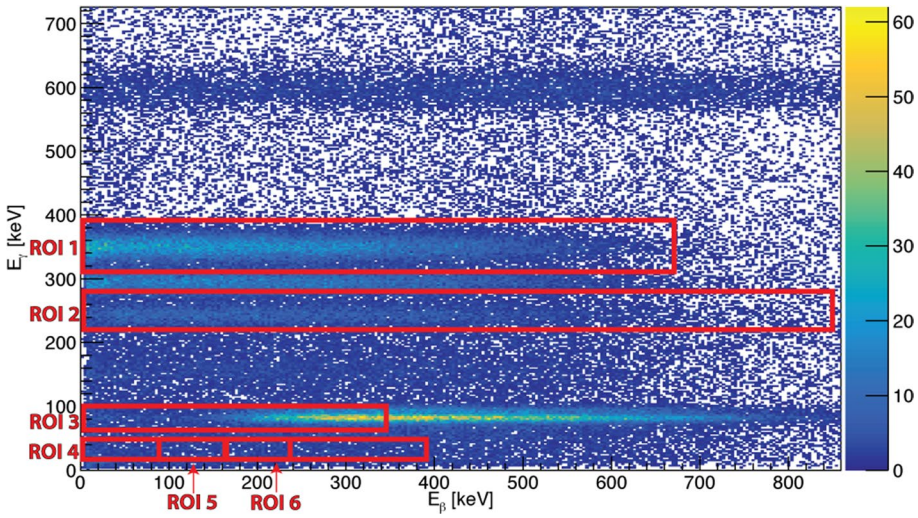

Fig. 1 A representative beta-gamma histogram using 7 ROIs where only ^{222}Rn is present in the measured sample. ROI 7 is not shown in this image since it is a combination of ROI 5 and ROI 6. (Color figure online)

until rejected through the gas processing. The rejection of radon of the systems is generally greater than 10^5 [6]. The amount of any isotope of radon can vary drastically by location due to emanation factors from the soil type, climate, and containment in man-made structures [5, 7–9]. Since radon levels vary geographically, it is uncertain what the appropriate level of radon rejection is needed for a system.

Although the majority of the radon is rejected during gas processing, periodically there are instances when radon will make it to the nuclear detectors and is present during the sample measurements. The prevailing nuclear measurement technique for radioxenon uses a coincidence measurement of the beta-gamma signature from the isotopic decay to identify the isotope and activity. The concentration and activity are calculated using the net-count method [6, 10, 11]. The primary sources of interfering backgrounds in the measurement are the radon daughters ^{214}Pb and ^{214}Bi, which decay via β^- decay. There are more daughters of radon that decay through β^- emission but the half-life ^{210}Pb is so large with respect to the measurement time that the remainder of the decay chain is considered inconsequential.

Radioxenon activities and activity concentrations are determined by the net-count method which relies on the counts in regions-of-interest (ROIs) of a two-dimensional beta-gamma energy histogram. There is no methodology in the net-count method to determine the activity of radon. Each ROI represents a unique coincidence decay of a xenon isotope with one ROI specified for counts emanating from ^{214}Pb (ROI 1). The ROIs are used to identify the highest intensity coincident beta-gamma decay peak for a nuclide. The net-count method uses interference terms in calculating activity to compensate for the additional counts coming from these lower intensity decays not associated with the isotope identified with that ROI (e.g., subtract out the expected radon counts from the specific xenon ROI). Unfortunately, these interferences can increase the uncertainty of the measurement and can be detrimental to the MDC of the system. The presence of radon introduces counts to all ROIs as seen in Fig. 1. Due to these interferences, it is possible for the radon to completely overwhelm all the radioxenon signatures.

It would be difficult to measure the activity of ^{222}Rn directly using the beta-gamma coincidence histogram but rather it can be inferred by the daughter isotopes. The decay of ^{222}Rn, ^{218}Po, and ^{214}Po is via alpha decay with a 5.49-MeV, 6.00-MeV, and 7.67-MeV alpha, respectively. The alphas are detected in the range of the traditional beta histogram but are not present in the beta-gamma coincidence histogram. The conversion electrons and gamma signatures directly from the decay of radon have low branching ratios as well. It could be possible to just use the gamma spectrum of the daughter nuclides to determine radon activity, but the gamma spectrum can sometimes be overwhelmed by background or xenon signatures. Therefore, the use of the beta-gamma coincidence data allows for a cleaner isolation of radon progeny and xenon signatures over background.

Simulation of ^{214}Pb and ^{214}Bi

The half-lives of ^{214}Pb and ^{214}Bi are relatively short and a pure measurement of each nuclide alone is impossible. Therefore, simulations were performed using Geant4 [12] to determine the contribution of the daughter nuclides to the background and ROI and are shown in Fig. 2. There are several beta-gamma detectors that have been developed or are currently under development. The gamma detectors are generally a NaI(Tl) detector with a well and the beta detector is typically a plastic scintillator with a cavity to hold the radioxenon sample. The detector geometry simulated was a 6-cc scintillating plastic beta cell inside of a NaI(Tl) well [13]. The simulation was performed for each nuclide that

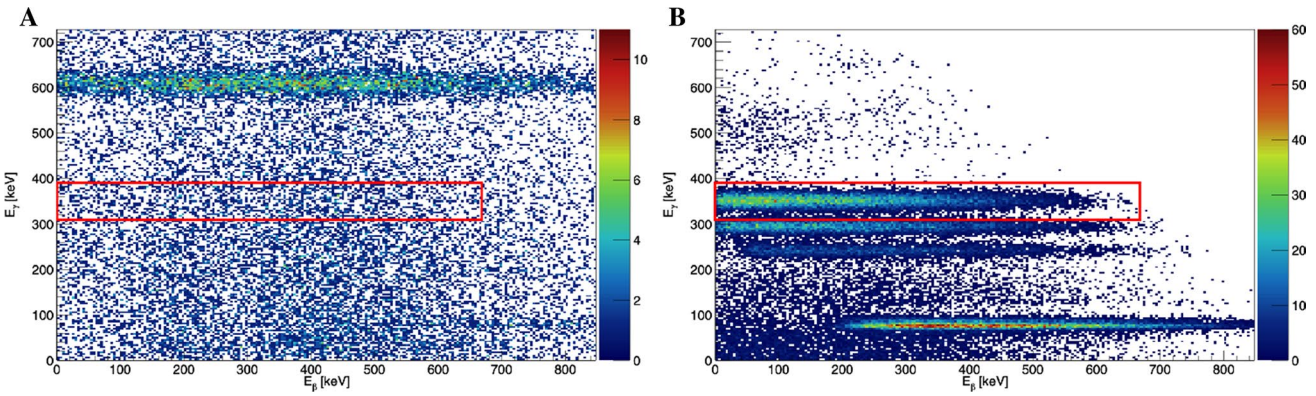

Fig. 2 GEANT4 simulation of ^{214}Bi (**A**) and ^{214}Pb (**B**) where the ROI 1 is outlined in red. (Color figure online)

decays via β^- decay (i.e., ^{214}Pb and ^{214}Bi) to distinguish each nuclide's features in a beta-gamma detector system. A total of 10^5 events were simulated for each isotope. This is the targeted number of events for a typical detector calibration [14].

The region of interest for radon determination is ROI 1 in the net-count method and is attributed to the daughter isotope ^{214}Pb. The net-count method has ROI 1 limits of 4–672 keV for the beta energy region and 310–390 keV for the gamma energy region. Since ^{214}Bi is the daughter nuclide of ^{214}Pb, and the measurement time is long compared to the half-life, for every ^{214}Pb decay there will be a corresponding ^{214}Bi decay in the detector. It can be seen from Fig. 2a. A that there are also counts from ^{214}Bi present in ROI 1. The simulation is used to determine the fractional abundance F of each daughter isotope and shows that 9.28% of the counts in ROI 1 emanate from ^{214}Bi (due to Compton down-scattering) and 90.72% of the total counts come from ^{214}Pb. These fractional abundances will not change unless there is a change in ROI limits.

Extending the absolute calibration method [14] to include ^{214}Pb or even using a calibrated radon source to determine the efficiency is challenging without the simulation to determine the number of counts of ^{214}Bi in ROI 1. Alternatively, efficiencies can be determined from the simulation or extrapolated from the radioxenon efficiencies. The experimental radioxenon efficiencies for this paper were taken from data analyzed with the absolute calibration method, fit with a function, and extrapolated to 352 keV (gamma) and averaged to 223 keV (beta). The simulation yielded an $\varepsilon^{Simulated} = 51.4\%$ while the experimental resulted in $\varepsilon^{Experimental} = 54.4\%$.

Activity of ^{222}Rn

An equation for the activity of radon can now be formulated using the abundance of the daughter isotopes[2] and the efficiency of the detector. The activity that is calculated in this paper is only a quantification of radon that makes it to the cell. The majority of radon in sampled whole air is rejected during processing therefore the total amount of activity and concentration of radon that was in an atmospheric sample will not be determined by this formula. If the radon rejection of the system is known, then the total activity of the radon that makes it to the detector cell can be used to determine the radon concentration that was in the sampled whole air. However, the radon rejection limit for most systems is just a lower limit. As stated previously, the initial abundance of radon daughters introduced to the beta cell is zero due to sample processing. Therefore, the expected counts observed in a beta-gamma histogram are due to daughter particles built-up over repeated processing cycles and decayed during the acquisition period. The number of total expected

[2] See the Supplementary information for more details on the abundance of the radon daughter calculations.

disintegrations ($\Delta C_{214_{Pb}}$) from ^{214}Pb over an acquisition time (T_A) is the integral of its activity as shown in

$$\Delta C_{214_{Pb}} = A_{222Rn}\big|_{t=0}\lambda_{214Pb}\left(\frac{1}{\lambda_{218Po}-\lambda_{222Rn}}\frac{\frac{\lambda_{218_{Po}}}{\lambda_{222Rn}}}{\lambda_{214Pb}-\lambda_{222Rn}}(1-e^{-\lambda_{222Rn}T_A})\right.$$
$$-\frac{1}{\lambda_{218Po}-\lambda_{222Rn}}\frac{1}{\lambda_{214Pb}-\lambda_{218Po}}(1-e^{-\lambda_{218_{Po}}T_A}) \quad (1)$$
$$\left.+\frac{1}{\lambda_{214Pb}-\lambda_{222Rn}}\frac{\frac{\lambda_{218_{Po}}}{\lambda_{214_{Pb}}}}{\lambda_{214Pb}-\lambda_{218Po}}(1-e^{-\lambda_{214_{Pb}}T_A})\right) = A_{222Rn}\big|_{t=0}B(T_A),$$

where λ is the decay constant of the nuclide and $B(T_A)$ is simply the terms in the parentheses multiplied by λ_{214Pb}. For a 12-h measurement and known half-lives, this value calculates to $B(T_A)=38{,}903.7$ s.

The total number of expected disintegrations from ^{214}Pb can be centralized to just the counts in ROI 1 by dividing the total counts by the efficiencies for ROI 1 and the branching ratios associated with the decays. The counts are then corrected for the additional presence of ^{214}Bi using the fractional abundance of ^{214}Pb ($F_{214_{Pb}}$=90.72%). The activity for radon (at the start of measurement) is then.

$$A_{222Rn}\Big|_{t=0}(Bq) = \frac{\Delta C_{214_{Pb}}}{B(T_A)} = \frac{\Delta C_{ROI1} * F_{214_{Pb}}}{\varepsilon_\gamma \varepsilon_\beta BR_\gamma BR_\beta * B(T_A)}, \quad (2)$$

where BR are the branching ratios associated with ^{214}Pb, BR_β is 100% and the BR_γ for the 351-keV emission is 35.6% [15], and ΔC_{ROI1} is deadtime corrected and background subtracted counts in ROI 1.[3] This analysis assumes there is no memory effect from a previous sample.[4] Memory-effect is the presence of residual activity of radon or xenon that has diffused into the detector from a previous measurement [16–18]. A gas-background measurement right before the sample measurement can be used to correct counts for memory effect. Next generation radioxenon systems use coated cells to mitigate any memory effect.

Calculating radon rejection levels for radioxenon MDC

The MDCs were calculated for all radioxenon isotopes over a simulated range of radon activities. Each activity of radon simulated correlated to a different radon rejection level. The MDC for each radioxenon isotope relies on a well-calibrated detector (i.e., interference terms and efficiencies). The interference ratios are the contribution of one isotope of xenon or radon to another ROI not associated with that isotope. The radon (^{214}Pb) interference terms are calculated as the ratio of the number of counts in the ROIs to ROI 1. The interference ratios should not change regardless of activity levels.

A set of measurements can be obtained experimentally with the detector to measure MDC levels. They consist of a sample measurement with only stable xenon present, a gas background, and a detector background. This data is needed to determine the baseline MDC levels for xenon. The MDC is back calculated to the time of collection for each xenon isotope [19]. The contribution due to the interference is attributed to either counts from radon, ^{135}Xe, or ^{133}Xe in the other ROIs. Without the presence of radioxenons or memory effect, the dominating term for MDCs is the contribution from the background. The MDC will start to increase as more radon is introduced into a measurement. Identifying the radon activity at which the xenon MDCs are dominated by radon interference can allow system developers and users to know if the system's radon rejection is sufficient for its location and performance metrics instead of striving for higher radon rejection values.

To determine the radon rejection level required for a system in a specific location, a simulated radon activity can be used to determine the expected additional counts in ROI 1 due to radon using Eq. (2) into the stable xenon sample measurement. Additional counts are introduced to the other ROIs using the interference ratios that were measured for a system. The MDC for each xenon isotope is then calculated as.

$$\mathrm{MDC}_{Xe}(mBq) = \frac{2.71+4.65\sigma_0}{\varepsilon_\gamma \varepsilon_\beta BR_\gamma BR_\beta}\frac{1000\lambda T_C}{(1-e^{-\lambda T_C})e^{-\lambda T_P}(1-e^{-\lambda T_A})V_{Air}}, \quad (3)$$

where σ_0 is the uncertainty of the measurement from the sample, gas, and detector measurements, λ is the decay constant per isotope, V_{Air} is the volume of air, and T is the time for collection (C), processing (P), and acquisition (A) [6]. The uncertainty equation used for this MDC calculation is $\sigma_0^2 = \mu_I+\mu_M+\mu_B+\sigma_I^2+\sigma_M^2+\sigma_B^2$ where μ is the mean net

[3] An equation for MDA can be found in the Supplementary information.

[4] See Supplementary information for more information on the consideration of memory effect.

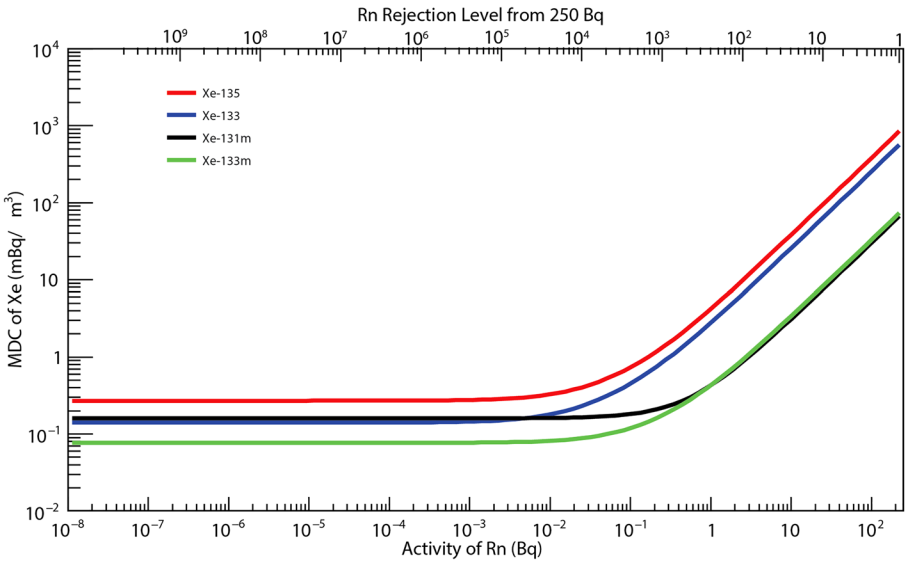

Fig. 3 Radioxenon MDC values for a sample with an initial activity of 250 Bq over a range of radon rejections. The MDC values were calculated for a complete (blank) sample measurement set (background, gas background, sample) without radioxenon present with a range of simulated radon activities. (Color figure online)

counts and σ is the uncertainty associated with the interference (I), memory (M), and background (B).

An exercise of this calculation would be to determine the impact to MDCs if 250 Bq of radon was collected by a system during a typical collection run without any radon rejection. Then, the radon rejection can be incrementally increased to determine at what radon activity and radon rejection level is needed to no longer impact the sensitivities. For this example, a total of 1.62 cc of xenon was placed into the cell, corresponding to a sampling of 18.64 m^3 of whole atmospheric air (assuming 0.087 m^3 of air per cc of xenon). The calculated MDC for each isotope of radioxenon for activity and radon rejection level can be seen in Fig. 3 for the example with 250 Bq of activity for radon. A general trend is seen on the right-hand side of the results where the interference from the radon dominates the uncertainty term in the MDC equation ($\mu_I > \mu_M + \mu_B$). As lower radon activities decrease, the uncertainty becomes dominated by any memory effect and the background and curves out to an almost flat line.

These measurements, simulations, and calculations can be repeated for any atmospheric monitoring system. Further, the starting radon activity level, radon rejection level, and xenon quantity can be varied to match the system and location. The level of radon rejection needed for a system can then be matched to meet the requirements of the system's sensitivities.

Discussion and conclusion

The MDC values for the four radioxenon isotopes of interest in this detector setup and the above example with a starting radon activity of 250 Bq show that a radon rejection level of 10^5 is sufficient to limit impact on the sensitivity of the detector. The radon activity would have to be an order of magnitude or larger than 250 Bq to impact the results seen above. The activity of radon collected is dependent on the concentration in atmospheric air sampled as well as the amount of air sampled by the system. Atmospheric radon levels vary both geographically and seasonally, but local levels can be easily surveyed by radon detectors such as a DURRIDGE RAD7. If the radon rejection level of a system is well known and quantified, it would be possible to determine the concentration of radon that is present in the atmosphere. Next-generation atmospheric monitoring systems that can sample higher amounts of air will have higher amounts of radon collected. A higher radon rejection level may be needed for these systems.

This paper detailed a method to determine the activity of radon in a beta-gamma detector using coincidence measurements and the net-count methodology. Radon activity levels can now be calculated from ROI 1 counts and tracked as part of atmospheric monitoring. Radon rejection level requirements for radioxenon sampling systems can also be determined based on location and expected radon levels using the method outlined in this paper. Increases in radon activities

seen in the detector cell can serve as a system performance monitor indicating a failure in the radon rejection process of that atmospheric sampling system.

Supplementary Information The online version contains supplementary material available at https://doi.org/10.1007/s10967-022-08480-1.

Acknowledgements We would like to thank the DOE for sponsorship of this work; U. S. Department of Energy, Office of Nonproliferation and National Security, Office of Research and Development. Any subjective views or opinions that might be expressed in the paper do not necessarily represent the views of the U.S. Department of Energy or the United States Government.

References

1. Ringbom A, Larson T, Axelsson A, Elmgren K, Johansson C (2003) SAUNA—a system for automatic sampling, processing, and analysis of radioactive xenon. Nucl Instrum Methods Phys Res Sect A Accel Spectrometers Detect Assoc Equip 508(3):542–553
2. Bowyer TW et al (1998) Automated separation and measurement of radioxenon for the Comprehensive Test Ban Treaty. J Radioanal Nucl Chem 235(1–2):77–82
3. Prelovskii VV, Kazarinov NM, Donets AY, Popov VY, Popov IY, Skirda NV (2007) The ARIX-03F mobile semiautomatic facility for measuring low concentrations of radioactive xenon isotopes in air and subsoil gas. Instrum Exp Tech 50(3):393–397
4. Le Petit G et al (2008) Contribution to the development of atmospheric radioxenon monitoring. J Radioanal Nucl Chem 276(2):391–398
5. UNSCEAR (2010) Sources and effects of ionizing radiation United Nations Scientific Committee on the Effects of Atomic Radiation, vol I, no. c.
6. Cooper MW et al (2019) Radioxenon net count calculations revisited. J Radioanal Nucl Chem 321(2):369–382
7. Burnett JL, Croudace IW, Warwick PE (2010) Short-lived variations in the background gamma-radiation dose. J Radiol Prot 30(3):525–533
8. Nazaroff WW, Nero AV (1988) Radon and its decay products in indoor air. Wiley, New York
9. Nero AV, Gadgil AJ, Nazaroff WW, Revzan KL (1990) Indoor radon and decay products: Concentrations, causes, and control strategies. Berkeley, DOE/ER-0480P
10. Axelsson A, Ringbom A (2003) Xenon air activity concentration analysis from coincidence data. Stockholm, Sweden, FOI-R--0913--SE
11. Axelsson A, Ringbom A (2014) On the calculation of activity concentrations and nuclide ratios from measurements of atmospheric radioactivity. Appl Radiat Isot 92:12–17
12. Agostinelli S et al (2003) Geant4—a simulation toolkit. Nucl Instrum Methods Phys Res Sect A Accel Spectrometers Detect Assoc Equip 506(3):250–303
13. Cooper MW et al (2007) Redesigned β–γ radioxenon detector. Nucl Instrum Methods Phys Res Sect A Accel Spectrometers Detect Assoc Equip 579(1):426–430
14. Cooper MW, Ely JH, Hayes JC, Mayer MF, McIntyre JI, Slack JL (2019) β–γ absolute calibration. Richland, WA, PNNL-27572 Rev. 1
15. Wu S-C (2009) Nuclear data sheets for A = 214. Nucl Data Sheets 110(3):681–748
16. Seifert CE, et al. (2005) Mitigation of memory effects in beta scintillation cells for radioactive gas detection. In: Proc. 27th Seism. Res. Symp. Ground-Based Nucl. Explos. Monit. Technol., pp 804–814
17. Bläckberg L et al (2013) Memory effect, resolution, and efficiency measurements of an Al2O3 coated plastic scintillator used for radioxenon detection. Nucl Instrum Methods Phys Res Sect A Accel Spectrometers Detect Assoc Equip 714:128–135
18. Yongchun X et al (2017) Studies on adsorption-desorption of xenon on surface of BC-404 plastic scintillator based on soaking method. Nucl Instrum Methods Phys Res Sect A Accel Spectrometers Detect Assoc Equip 847:99–103
19. Cooper MW, Hayes JC, Schrom BT, Ely JH, McIntyre JI (2016) Minimum detectable concentration and concentration calculations. Richland, WA, PNNL-25418
20. Currie LA (1968) Limits for qualitative detection and quantitative determination. Application to radiochemistry. Anal Chem 40(3):586–593